Mon. Not. R. Astron. Soc. **282,** 1330–1342 (1996)

APM $z \gtrsim 4$ survey: distribution and evolution of high column density H I absorbers

L. J. Storrie-Lombardi,[1★] M. J. Irwin[2] and R. G. McMahon[1]

[1]*Institute of Astronomy, Madingley Road, Cambridge CB3 0HA*
[2]*Royal Greenwich Observatory, Madingley Road, Cambridge CB3 0EZ*

Accepted 1996 June 7. Received 1996 June 6; in original form 1995 November 29

ABSTRACT

Eleven candidate damped Lyα absorption systems were identified in 27 spectra of the quasars from the APM $z \gtrsim 4$ survey covering the redshift range $2.8 \leq z_{\rm absorption} \leq 4.4$ (eight with $z_{\rm absorption} > 3.5$). High-resolution echelle spectra (0.8-Å FWHM) have been obtained for three quasars, including two of the highest redshift objects in the survey. Two damped systems have confirmed H I column densities of $N_{\rm H\,I} \geq 10^{20.3}$ atom cm^{-2}, with a third falling just below this threshold. We have discovered the highest redshift damped Lyα absorber known at $z = 4.383$ in QSO BR 1202 – 0725.

The APM QSOs provide a substantial increase in the redshift path available for damped surveys for $z > 3$. We combine this high-redshift sample with other quasar samples covering the redshift range $0.008 < z < 4.7$ to study the redshift evolution and the column density distribution function for absorbers with $\log N_{\rm H\,I} \geq 17.2$. In the H I column density distribution $f(N) = kN^{-\beta}$ we find evidence for breaks in the power law, flattening for $17.2 \leq \log N_{\rm H\,I} \lesssim 21$ and steepening for $\log N_{\rm H\,I} > 21.2$. The breaks are more pronounced at higher redshift. The column density distribution function for the data with $\log N_{\rm H\,I} \geq 20.3$ is better fitted with the form $f(N) = (f_*/N_*)(N/N_*)^{-\beta} \exp(-N/N_*)$ with $\log N_* = 21.63 \pm 0.35$, $\beta = 1.48 \pm 0.30$, and $f_* = 1.77 \times 10^{-2}$. We study the evolution of the number density per unit redshift of the damped systems by fitting the sample with the customary power law $N(z) = N_0(1+z)^{\gamma}$. For a population with no intrinsic evolution in the product of the absorption cross-section and comoving spatial number density this will give $\gamma = 1/2$ ($\Omega = 1$) or $\gamma = 1$ ($\Omega = 0$). The best maximum-likelihood fit for a single power law is $\gamma = 1.3 \pm 0.5$ and $N_0 = 0.04^{+0.03}_{-0.02}$, consistent with no intrinsic evolution even though the value of γ is also consistent with that found for the Lyman limit systems where evolution is detected at a significant level. However, redshift evolution is evident in the higher column density systems with an apparent decline in $N(z)$ for $z > 3.5$.

Key words: galaxies: evolution – galaxies: formation – quasars: absorption lines – quasars: individual: BR 1033 – 0327, BRI 1108 – 0747, BR 1202 – 0725 – cosmology: miscellaneous.

1 INTRODUCTION

This paper is the third of a series presenting results from studies of the QSOs discovered in the APM survey for $z \gtrsim 4$ quasars. A study of the evolution of Lyman-limit absorption systems over the redshift range $0.04 \leq z \leq 4.7$ was presented in Storrie-Lombardi et al. (1994, hereafter Paper I). The intermediate-resolution (5 Å) QSO spectra and the survey for high-redshift damped Lyα absorbers are presented in Storrie-Lombardi et al. (1996, hereafter Paper II). The evolution of the cosmological mass density of neutral gas at high redshift and the implications for galaxy formation theories are discussed in Storrie-Lombardi, McMahon & Irwin (1996, hereafter Paper IV). In separate papers we will describe the intrinsic properties of the QSOs and studies of

★Present address: Carnegie Observatories, 813 Santa Barbara Street, Pasadena, CA 91101, USA.
E-mail: lisa@ociw.edu (LJSL); mike@ast.cam.ac.uk (MJI); rgm@ast.cam.ac.uk (RGM)

the Lyα forest clouds at high redshift. A high-resolution study of the Lyα forest region in a redshift $z=4.5$ QSO has been completed by Williger et al. (1994).

How and when galaxies formed are questions at the forefront of work in observational cosmology. Absorption systems detected in quasar spectra provide the means to study galaxy formation and evolution up to redshifts $z\approx 5$, back to when the Universe was less than 10 per cent of its present age. Surveys for absorption features have several advantages over trying to detect galaxies directly at high redshift. Much shorter exposure times are required, because the QSOs are relatively bright ($R\approx 18$–19.5) and the large equivalent width systems are easily detected in the spectra. This provides good absorption candidates to follow up with higher resolution spectra. The redshift and column density can be accurately determined from the wavelength of the absorption system and the line profile. This is far easier and more reliable than trying to obtain a spectrum of a very faint high-redshift galaxy directly.

While the baryonic content of spiral galaxies that are observed in the present epoch is concentrated in stars, in the past this must have been in the form of gas. The principal gaseous component in spirals is neutral hydrogen, and this has led to surveys for absorbers detected by the damped Lyα lines they produce (Wolfe et al. 1986, hereafter WTSC; Lanzetta et al. 1991, hereafter LWTLMH; Lanzetta, Wolfe & Turnshek 1995, hereafter LWT; Wolfe et al. 1995; Paper II). Although damped Lyα systems are observationally very rare objects, with ~ 40 confirmed examples known, the H I mass per unit comoving volume they contain is roughly comparable to the mass density of baryonic matter in present-day spirals, i.e., a major constituent of the Universe (Wolfe 1987; LWT). Their metal abundances are much lower than Galactic values (Pettini, Boksenberg & Hunstead 1990; Rauch et al. 1990; Pettini et al. 1994), and they are characterized by low molecular content and low, but not negligible, dust content (Fall, Pei & McMahon 1989; Pei, Fall & Bechtold 1991; Pettini et al. 1994), features consistent with an early phase of galactic evolution. They may be the progenitors of spiral galaxies like our own, and are clearly important for the study of the formation and evolution of galaxies. They have been detected across a very large redshift range $z\approx[0.5, 4.5]$, providing the means to pinpoint the epoch of formation of disc galaxies and study their evolution.

11 candidate damped Lyα absorption systems out of 32 measured Lyα features were identified in 27 spectra of the mainly non-BAL quasars from the APM $z\gtrsim 4$ survey (Paper II). The 11 candidates cover the redshift range $2.8\leq z_{\rm absorption}\leq 4.4$ (eight with $z_{\rm absorption}>3.5$) and have estimated column densities $N_{\rm H\,I}\geq 10^{20.3}$ atom cm^{-2}. In this paper the QSO BR 1144 − 0723 with a candidate absorber at $z=3.26$ is removed from further consideration in the sample. It has been observed with the Anglo-Australian Telescope at high resolution, and the damped candidate has been found to be all O VI absorption at $z=4.0$ (R. Hunstead, private communication). High-resolution echelle spectra (0.8-Å FWHM) were obtained by S. D'Odorico as part of the ESO key programme studying high-redshift quasars for four of the QSOs in the APM sample (BRI 0952 − 0115, BR 1033 − 0327, BRI 1108 − 0747 and BR 1202 − 0725). The signal-to-noise ratio for BRI 0952 − 0115 was very poor, but the other spectra have been used to confirm two Lyα features as damped, with another falling just below the $\log N_{\rm H\,I}\geq 20.3$ threshold. We have discovered the highest redshift damped Lyα absorber known at $z=4.383$ in QSO BR 1202 − 0725. The confirmation of the absorption systems is discussed in Section 2. These data have been combined with data from previous surveys (WTSC; LWTLMH; LWT) and the results for the Lyman limit systems obtained in Paper I to study the H I column density distribution for $\log N_{\rm H\,I}>17.2$ and redshift evolution of these systems for $0.008<z<4.7$.

Numerous authors have studied the distribution of column densities, $f(N_{\rm H\,I})$, for Lyα absorption lines. The first determination was by Carswell et al. (1984) for lines with $10^{13}<N_{\rm H\,I}<10^{16}$ atom cm^{-2}. They found $f(N)\propto N^{-\beta}$ ($\beta=1.7\pm 0.1$). Damped Lyα absorption (DLA) systems comprise the high column density tail of neutral hydrogen absorbers with column densities of $N_{\rm H\,I}\geq 2\times 10^{20}$ atom cm^{-2}. They dominate the baryonic mass contributed by H I. When damped systems are included in the column density distribution function for a single power-law fit, the exponent is $\beta=1.4$–1.7 (cf. Tytler 1987; Petitjean et al. 1993, and references therein). Assuming that the baryonic mass is proportional to the H I column density and takes the form $f(N_{\rm H\,I})\propto N^{-\beta}$ for the H I column density distribution function, the mass contribution from the damped systems can be estimated as

$$M_{\rm total}\propto\int_{N_1}^{N_2} N_{\rm H\,I} f(N_{\rm H\,I})\,{\rm d}N_{\rm H\,I}$$

$$\propto\int_{N_1}^{N_2} N^{-\beta}N\,{\rm d}N \qquad \text{(assume } \beta\neq 2\text{)}$$

$$\propto\frac{1}{2-\beta}\,(N_2^{2-\beta}-N_1^{2-\beta}). \qquad (1)$$

One problem with the power-law representation is that if $\beta<2$, as all current estimates indicate, then the total mass in damped systems diverges unless an upper bound to the H I column density is assumed. For example, if we take $20.3\lesssim\log N_{\rm H\,I}\lesssim 22$, the fractional contribution to the total H I mass for damped systems, $M_{\rm f}$, is then $M_{\rm f}=0.86$ for $\beta=1.5$ and $M_{\rm f}=0.69$ for $\beta=1.7$. However, there is no a priori reason for assuming this upper limit, and hence there is no strict upper bound to any estimate of the total H I mass in damped systems. An alternative parametrization using a gamma function to describe the H I column density distribution was adopted by Pei & Fall (1995) and provides an elegant solution to the diverging mass problem. We discuss these points in more detail in Section 3, and the redshift evolution of the absorbers in Section 4.

2 CONFIRMATION OF DAMPED Lyα SYSTEMS

2.1 Echelle observations

Echelle spectra of four QSOs were obtained in 1993 March by S. D'Odorico as part of an ESO key programme studying high-redshift quasars. They were taken at La Silla with the

3.5-m NTT telescope using the EMMI instrument in echelle mode with a 2048×2048 pixel LORAL CCD as the detector. A slit 15 arcsec in length was used, and generally the slit width was 1.2 arcsec. Two grating set-ups were used, one covering 4700–8300 Å and the other covering 5800–9500 Å with a resolution of ~ 40 km s^{-1} (1 Å). (See Giallongo et al. 1994 for more details.) The observations are summarized in Table 1.

The spectra were extracted and calibrated using the OPTEXT routines[1] in conjunction with IRAF. The final flux-calibrated spectra agreed well with the existing 5-Å spectra (Paper II), except in the case of BRI 0952 – 0115 where the signal-to-noise ratio was very poor and the relative flux different by a factor of 2. This spectrum has been excluded from further analysis. Though not of exceedingly high quality, the spectra were suitable for fitting the damped Lyα candidates.

2.2 Fitting the damped candidates

The damped candidate system profiles were fitted using the vpgti[2] Voigt profile fitting software. The program requires three input spectra: the object, the errors and the continuum. The OPTEXT routines used in the reduction created the first two, and the continuum spectra were created by using continuum fits for the WHT spectra (Paper II) and extrapolating them to the echelle spectra, as was done in Williger et al. (1994). The centroids of the Lyα features were determined from narrow metal lines (e.g., O I, C II), and then the Lyα lines were fitted in a region 50–100 Å around the candidate feature. Generally, candidate damped systems seen in the low-resolution spectra appeared much stronger than they actually are, due to blending of the dense Lyα forest lines at low resolution. In all three QSOs the candidate damped systems are seen at higher resolution to break up into multiple overlapping components. The complexity of the blend, coupled with residual uncertainty in the exact placing of the continuum level, causes some of the error estimates from VPFIT to be somewhat optimistic. In particular, for BRI 1108 – 0747 and BR 1202 – 0725, numerical simulations suggest that an error in $\log N_{\rm H\,I}$ of $\sigma = 0.15$ should be adopted. The fitted lines are summarized in Table 2.

BR 1033 – 0327 ($z_{\rm em} = 4.509$, $z_{\rm absorption} = 4.15$)

The absorption candidate at $z = 4.15$ had been previously studied (Williger et al. 1994) with a 12 km s^{-1} echelle spectrum taken at CTIO. Their spectrum covered only the blue wing of the system, and from this the column density was estimated to be no greater than 3×10^{20} atom cm^{-1}. With spectral coverage of the entire absorber it is seen to be a complex system of at least five absorbers with a total column density of $\log N_{\rm H\,I} = 20.15 \pm 0.11$ atom cm^{-2} ($N_{\rm H\,I} = 1.4 \times 10^{20}$). In Paper II the column density was estimated to be $\log N_{\rm H\,I} = 20.2$. The redshifts of the Lyα absorbers were determined from five tentatively identified O I 1302 lines in the CTIO spectrum. The signal-to-noise ratio in the order where the Lyβ lines lie was too low to use in the fit. The spectrum with the best-fitting line profiles and $\pm 1\sigma$ fits are shown as solid lines in Fig. 1(a). The error array and normalized continuum are shown as dotted and dashed lines, respectively. The small spike at ≈ 6270 Å is real. It also appears in the 5-Å resolution spectrum (Paper II).

BRI 1108 – 0747 ($z_{\rm em} = 3.922$, $z_{\rm dla} = 3.607$)

The absorber at $z = 3.61$ is barely damped with a column density of $\log N_{\rm H\,I} = 20.33 \pm 0.15$ atom cm^{-2}. In Paper II we estimated the column density to be $\log N_{\rm H\,I} = 20.2$, so this system was not originally in the statistical sample. Several of the absorbers in the survey in Paper II have estimated column densities near the statistical sample threshold of $\log N_{\rm H\,I} = 20.3$. We expect some to be confirmed above this value and some below. The profile fit and $\pm 1\sigma$ fits are shown in Fig. 1(b). The redshift centroid was determined from a single strong C II 1334 line.

BR 1202 – 0725 ($z_{\rm em} = 4.694$, $z_{\rm dla} = 4.383$)

The damped system in this QSO has a column density of $\log N_{\rm H\,I} = 20.49 \pm 0.15$. It is the highest redshift damped Lyα system known. The ESO spectrum is shown with the profile fit and $\pm 1\sigma$ fits in Fig. 1(c). It was also measured in a higher resolution spectrum taken at CTIO (Wampler et al. 1996),

Table 1. ESO observations 1993 March.

QSO	Date (UT)	Exp (secs)	Grating	Slit (")
BRI0952 – 0115	93 Mar 14	5400	GR9CD3	1.2
	93 Mar 14	7200	GR9CD3	2.0
BR 1033 – 0327	93 Mar 15	7200, 8000	GR9CD3	1.2
BRI1108 – 0747	93 Mar 15	6000	GR9CD3	1.2
	93 Mar 15	6000	GR9CD4	1.2
BR 1202 – 0725	93 Mar 14	8000	GR9CD3	1.2
	93 Mar 15	6797	GR9CD3	1.2
	93 Mar 15	7200, 8000	GR9CD4	1.2

Table 2. Lyman α absorption systems.

QSO	Absorption Redshift	log $N_{\rm HI}$
BR1033 – 0327	4.14945	19.80 ± 0.10
	4.15314	18.69 ± 0.30
	4.16647	19.70 ± 0.15
	4.16726	19.37 ± 0.42
	4.17481	19.60 ± 0.24
BRI1108 – 0747	3.60673	20.33 ± 0.15
BR1202 – 0725	4.38290	20.49 ± 0.15

[1]These routines were written by Bob Carswell, Jack Baldwin and Gerry Williger for the reduction of CTIO echelle data.
[2]Written by R. F. Carswell, J. K. Webb, A. J. Cooke and M. J. Irwin; see also Cooke (1994).

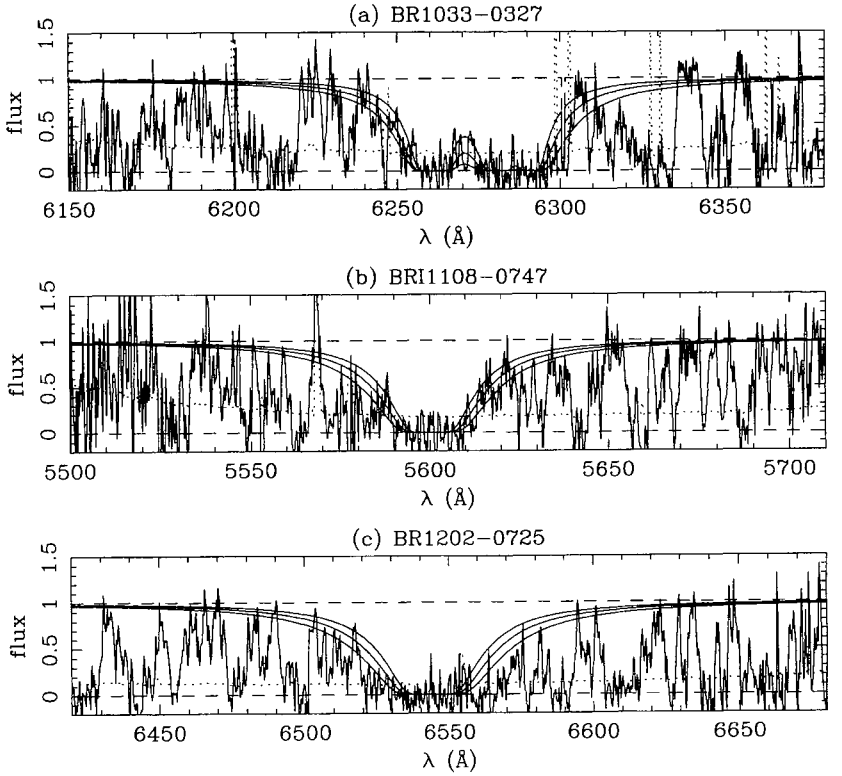

Figure 1. The profile fit and $\pm 1\sigma$ fits to the damped Lyα absorbers are shown as solid lines. The error arrays are shown as dotted lines. The components are listed in Table 2. (a) The H I absorption complex in BR 1033 − 0327 at $z=4.15$ is a system of at least five absorbers with a total column density of $\log N_{\rm H\,I}=20.15\pm0.11$ atom cm^{-2}. (b) The damped Lyα absorber in BRI 1108 − 0747 at $z=3.607$ with $\log N_{\rm H\,I}=20.33\pm0.15$ atom cm^{-2}. (c) The damped Lyα absorber in BR 1202 − 0725 at $z=4.383$. This is the highest redshift damped Lyα absorber known. The central damped component is shown with $\log N_{\rm H\,I}=20.49\pm0.15$.

and includes over 10 components. Lu et al. (1996) have observed it at Keck with HIRES, and measure a column density of $\log N_{\rm H\,I}=20.6\pm0.1$. It was estimated in Paper II to have a column density of $\log N_{\rm H\,I}=20.5$.

The status of the systems detected in the APM damped Lyα absorption survey is summarized in Table 3. (It is an updated version of table 7 from Paper II.) Those marked with an asterisk have column densities $\log N_{\rm H\,I}\geq20.3$ atom cm^{-2} and make up the statistical sample of high-redshift absorbers used in the analysis. In Paper IV this data set is combined with previous surveys to study the evolution of the cosmological mass density of neutral gas at high redshift, and the implications for galaxy formation theories are discussed.

3 THE H I COLUMN DENSITY DISTRIBUTION FOR LOG$N_{\rm H\,I}>17.2$

3.1 Background

The distribution of the H I column densities for QSO absorption-line systems has been investigated by several authors. Tytler (1987) found that the distribution may be represented by a single power law $f(N)\propto N^{-\beta}$ over the range $13.3\leq\log N_{\rm H\,I}\leq21.8$ with $\beta=1.51\pm0.02$. He argued that this was evidence for a single population. Fitting the higher and lower column density systems separately, Tytler found $\beta=1.61\pm0.10$ for $\log N_{\rm H\,I}<16.7$ and $\beta=1.35\pm0.07$ for $\log N_{\rm H\,I}>17.2$, very similar slopes particularly considering the inadequacies of the data set. Sargent et al. (1980) found a single-power-law fit over the entire column density range, but noted that since little detailed data was available for $15.5\leq\log N_{\rm H\,I}\leq17.2$, the region where the H I becomes optically thick, this was not evidence for a single population. They also found $\beta=1.39$ for $\log N_{\rm H\,I}\geq17.3$. LWTLMH found the best fit for the high column density data ($17.2\leq\log N_{\rm H\,I}\leq21.8$) gave $\beta=1.25$. All of these values for β agree within the errors. Petitjean et al. (1993) reviewed these results and concluded that neither a single nor double power-law fitted well for $13.3\leq N_{\rm H\,I}\leq21.8$, but that there clearly was a flattening of the distribution function around $\log N_{\rm H\,I}\approx16$.

Looking at the damped Lyα systems alone ($20.3\leq N_{\rm H\,I}\leq21.8$), LWTLMH found $\beta=1.73$. Most investigators find no evidence for any substantial redshift evolution in the distribution function, although LWT find an increased number of the highest column density systems at high redshift. Into this quagmire we wade with the absorption systems from the APM Damped Lyα Survey (Paper II) and the results for the Lyman-limit system evolution from Paper I to attempt to better quantify what is happening with the high column density H I at high redshift.

Table 3. Status of absorbers in APM damped Lyman α absorption survey.

QSO	z_{min}	z_{max}	z_{em}	z_{dla}	W_{rest} Å	log N_{HI} estimate	log N_{HI} actual
BR 0019 – 1522	2.97	4.473	4.528	3.42	7.6	20.0	
				3.98	12.3	*20.5	
				4.28	8.0	20.1	
BRI0103 + 0032	2.87	4.383	4.437	4.23	5.8	19.8	
BRI0151 – 0025	2.74	4.142	4.194				
BRI0241 – 0146	2.86	4.002	4.053	3.41	5.7	19.8	
BR 0245 – 0608	2.96	4.186	4.238				
BR 0351 – 1034	3.09	4.297	4.351	3.62	6.6	19.9	
				4.14	6.3	19.9	
BR 0401 – 1711	2.82	4.184	4.236				
BR 0951 – 0450	2.93	4.315	4.369	3.84	24.0	*21.0	
				4.20	10.6	*20.3	
BRI0952 – 0115	2.99	4.372	4.426	4.01	18.0	*20.8	
BRI1013 + 0035	2.61	4.351	4.405	3.10	17.5	*20.8	
				3.73	9.6	20.2	
				4.15	7.4	20.0	
BR 1033 – 0327	2.91	4.454	4.509	4.15	9.6	20.2	20.15 ± 0.11
BRI1050 – 0000	2.83	4.233	4.286				
BRI1108 – 0747	2.64	3.873	3.922	2.79	8.3	20.1	
				3.607	9.0	20.2	*20.33 ± 0.15
BRI1110 + 0106	2.58	3.869	3.918	3.25	5.2	19.7	
				3.28	6.2	19.9	
BRI1114 – 0822	3.19	4.440	4.495	3.91	6.7	19.9	
				4.25	11.7	*20.4	
				4.45	5.3	19.7	
BR 1144 – 0723	Removed from sample.						
BR 1202 – 0725	3.16	4.637	4.694	3.20	5.4	19.7	
				3.38	7.1	20.0	
				4.13	7.8	20.1	
				4.383	13.2	20.5	*20.49 ± 0.15
BRI1328 – 0433	2.24	4.165	4.217	3.08	8.3	20.1	
BRI1335 – 0417	3.08	4.342	4.396				
BRI1346 – 0322	2.65	3.942	3.992	3.15	6.8	19.9	
				3.36	5.0	19.7	
				3.73	10.0	*20.3	
BRI1500 + 0824	2.39	3.894	3.943	2.80	11.3	*20.4	
GB 1508 + 5714	2.73	4.230	4.283				
MG 1557 + 0313	2.66	3.842	3.891				
GB 1745 + 6227	2.47	3.852	3.901				
BR 2212 – 1626	2.69	3.940	3.990				
BR 2237 – 0607	2.96	4.502	4.558	4.08	11.5	*20.4	
BR 2248 – 1242	2.94	4.109	4.161				

*These absorbers are above the statistical sample threshold of $N_{H_I} \geq 2 \times 10^{20}$ atom cm^{-2}.
z_{min} = minimum redshift at which a DLA could be observed.
z_{em} = emission redshift of the QSO.
z_{max} = 3000 km s^{-1} blueward of z_{em}.
z_{dla} = redshift at which a damped candidate was observed.

3.2 A power-law distribution function

The form of the power-law column density distribution function $f(N)$ typically used is

$$f(N) = kN^{-\beta}. \quad (2)$$

$f(N)\,dN\,dX$ is defined as the number of absorbers in an absorption distance interval dX with H I column density N in the range $N + dN$. The absorption distance X is used to remove the redshift dependence in the sample and to put everything on a comoving coordinate scale, since $\Delta z = 0.5$ at redshift 2 is not the same as $\Delta z = 0.5$ at redshift 4. If the population of absorbers is non-evolving (i.e., their number density multiplied by their cross-section does not change with redshift), the absorption distance can be defined as

$$X(z) = \int_0^z = (1+z)(1+2q_0z)^{-1/2}\,dz; \quad (3)$$

therefore

$$X(z)=\begin{cases}\frac{2}{3}[(1+z)^{3/2}-1] & \text{if } q_0=0.5,\\ \frac{1}{2}[(1+z)^2-1] & \text{if } q_0=0.\end{cases} \quad (4)$$

(Bahcall & Peebles 1969; cf. Tytler 1987). The value of q_0 has little effect on the slope of the column density distribution function. In the analysis below we have utilized $q_0=0.5$. To allow for redshift evolution, the distribution function is normally generalized as

$$f(N,z)=kN^{-\beta}(1+z)^{\gamma}. \quad (5)$$

The damped Lyα systems and candidates from the APM survey shown in Table 3 have been combined with previous surveys for damped Lyα systems (WTSC; LWTLMH; LWT), which results in a data set of 366 QSOs yielding 44 damped systems with $\log N_{\rm H\,I}\geq 20.3$ covering the redshift range $0.2\leq z\leq 4.4$. The total redshift path and absorption distance covered by the surveys is shown in Table 4. A maximum-likelihood technique, described in Appendix A, has been employed to find values for β and k to determine if a power-law fit describes the H I column density distribution for this sample. As already indicated, a disadvantage of a power-law model for the H I column density distribution of damped Lyα absorbers is the divergent nature of the integral mass contained in the systems. Since it is straightforward to generalize the maximum-likelihood method to alternative forms of the distribution, we explore in Section 3.6 an alternative parametrization based on a gamma distribution (cf. Pei & Fall 1995).

3.3 Results for a single power law

A single-power-law fit to the combined data set described above of the form in equation (5) with $q_0=0.5$ results in $\beta=1.74\pm0.12$ and $\log k=13.9\pm2.3$, with similar values for $q_0=0$ ($\beta=1.75$, $\log k=13.9$). The quoted error for the normalization constant k is large, because for a small change in the value of β, k can change by 2 orders of magnitude. These results are in good agreement with the results found by LWTLMH ($\beta=1.73\pm0.29$, $\log k=13.63\pm0.09$) and are plotted for the entire data set in Fig. 2. The data are binned for display purposes only, with the vertical error bars plotted at the mean column density for each bin. We will see in the next section that a single power law is not a good fit to the data.

Table 4. Redshift and absorption distance paths.

Data Set	Δz	ΔX ($q_0=0$)	ΔX ($q_0=0.5$)
$0<z<4.7$			
APM Damped Lyα Survey	36.1	162.3	76.5
WTSC + LWTLMH + LWT	203.4	602.1	344.8
Combined	239.5	764.4	421.3
$z>3$			
APM Damped Lyα Survey	30.5	141.2	65.5
WTSC + LWTLMH + LWT	13.0	54.6	26.7
Combined	43.5	195.8	92.2

3.4 Cumulative H I distribution

As shown in Paper I for the Lyman-limit system evolution, the arbitrary binning of the data for presentation in differential plots includes a subjective component that can mask exactly what is happening in the underlying data. A cumulative distribution plot is far better at revealing the true nature of the distribution, and this approach is now examined. The log of the cumulative number of damped Lyα systems detected versus $\log N_{\rm H\,I}$ is plotted in Fig. 3(a). A point for the expected number of Lyman-limit systems that would be detected down to $\log N_{\rm H\,I}=17.2$ is shown by a circled dot. This is calculated by integrating the number density per unit redshift $[N(z)=0.27(1+z)^{1.55}]$ over the redshift path covered by the n QSOs in the DLA sample, i.e.,

$$LLS_{\rm expected}\sum_{i=1}^{n}\int N(z)\,{\rm d}z=\sum_{i=1}^{n}\int_{z_{\rm min}}^{z_{\rm em}}N_0(1+z)^{\gamma}\,{\rm d}z$$

$$=\sum_{i=1}^{n}\int_{z_{\rm min}}^{z_{\rm em}}0.27\,(1+z)^{1.55}\,{\rm d}z. \quad (6)$$

It is obvious from Fig. 3(a) that a power law will not fit the entire column density range $17.2\leq\log N_{\rm H\,I}\leq 22$. A Kolmogorov–Smirnov (KS) test yields a probability of less than 10^{-7} that the fit represents the underlying data set. In Figs 3(b)–(d) the same distribution is overplotted with single-power-law fits for different values of β that were fitted to the graph by eye. (b) shows that $\beta=1.34$ will fit from the Lyman limit column density through the damped systems with $\log N_{\rm H\,I}\approx 21$, a flatter slope than the canonical 1.5–1.7 range. (c) shows that $\beta=1.69$ fits the damped distribution

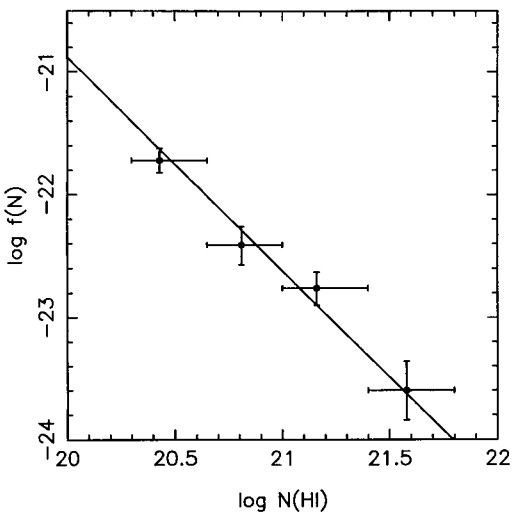

Figure 2. A single-power-law form of the column density distribution function, $f(N)=kN^{-\beta}$, fitted to the entire damped Lyα sample from the APM Damped Lyα Survey, WTSC, LWTLMH and LWT. The parameters of the fit are $\beta=1.74$ and $\log k=13.9$.

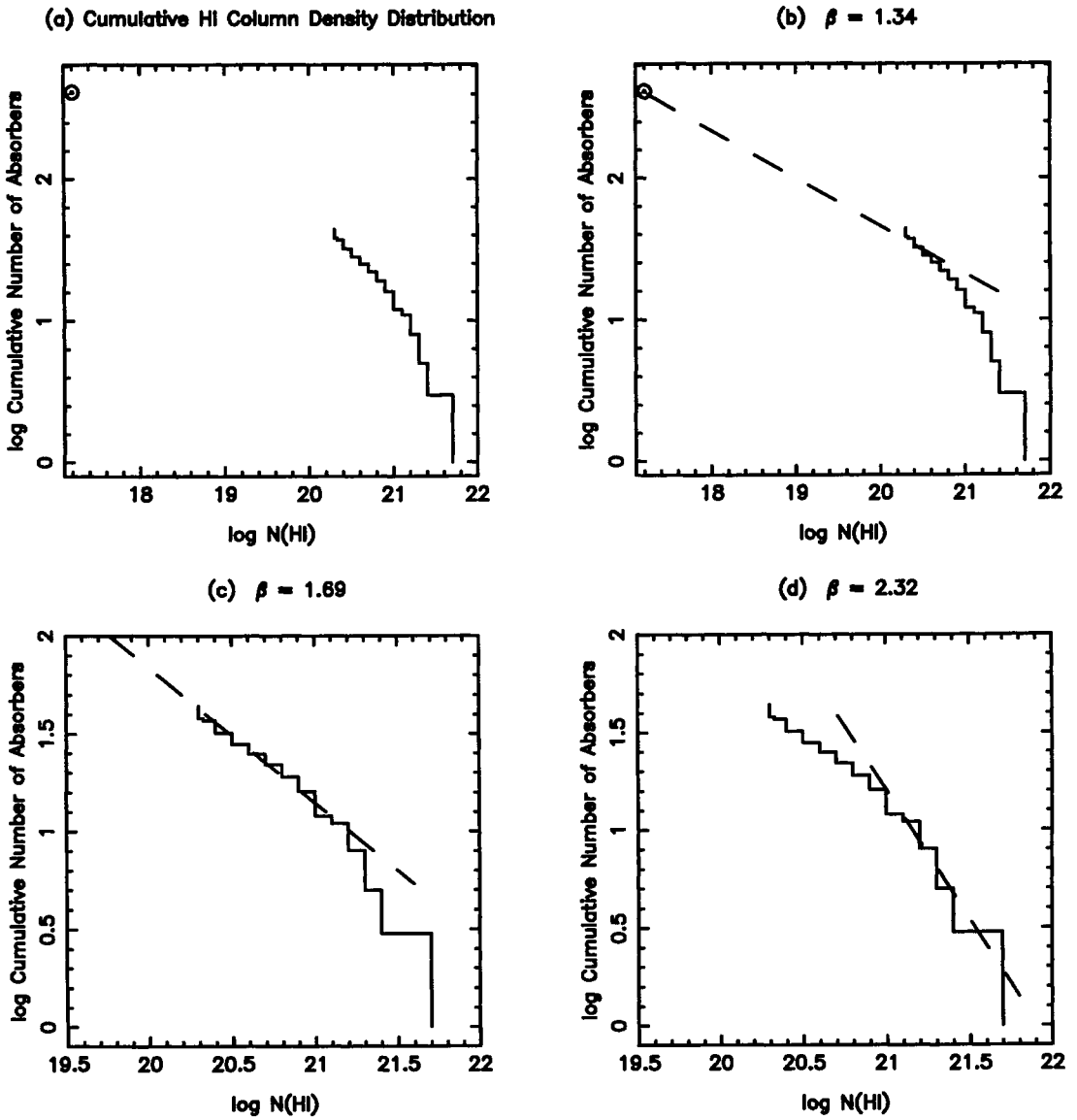

Figure 3. (a) The cumulative distribution for $17.2 \leq \log N_{\rm H_I} \leq 22$. The stepped line is the data for all the damped Lyα systems in the data set. The circled point is the number of Lyman-limit systems that would be expected, given the redshift path covered in the damped Lyα surveys. In (b)–(d) the same distribution is overplotted with single-power-law fits for different values of β that were fitted to the graph by eye. (b) shows that $\beta = 1.34$ will fit from the Lyman-limit column density through the damped systems with $\log N_{\rm H_I} \approx 21$, a flatter slope than the canonical $\beta \approx 1.5$–1.7 range. (c) Shows that $\beta = 1.69$ fits the systems with $20.3 \leq \log N_{\rm H_I} \leq 21.2$ well, but does not describe the high or low column density tails of the distribution. (d) Shows a fit to the sharp drop-off in numbers of damped systems with $\log N_{\rm H_I} \gtrsim 21$. This is evident from just looking at the estimated column densities for the damped systems in Table 3, or by looking at the spectra. There are not many heavily damped systems.

with $20.3 < \log N_{\rm H_I} < 21.2$ well, but does not describe the high or low column density tails of the distribution. (d) shows a fit to the sharp drop off in numbers for damped systems with $\log N_{\rm H_I} \geq 21$. This can be expected from looking at the estimated column densities for the damped systems in Table 3, or by looking at the spectra. There are not many heavily damped systems. Clearly, the results for a single-power-law fit depend critically on the range of column densities included. This characteristic can explain much of the variation in the results previously seen by various authors that were summarized in Section 3.1.

3.5 Redshift evolution for $0.008 < z < 4.7$

To qualitatively study the redshift evolution of the column density distribution of the damped Lyα systems the cumulative distribution shown in Fig. 3 has been split in half at redshift 2.5 and each set plotted individually (Fig. 4). The damped Lyα systems with $z > 2.5$ are shown by the solid line, and the absorbers with $z < 2.5$ are shown by the dashed line. The higher redshift absorbers appear to have a slightly flatter slope up to $\log N_{\rm H_I} = 21$ and then a sharper drop in the number of very high column density systems, although a KS

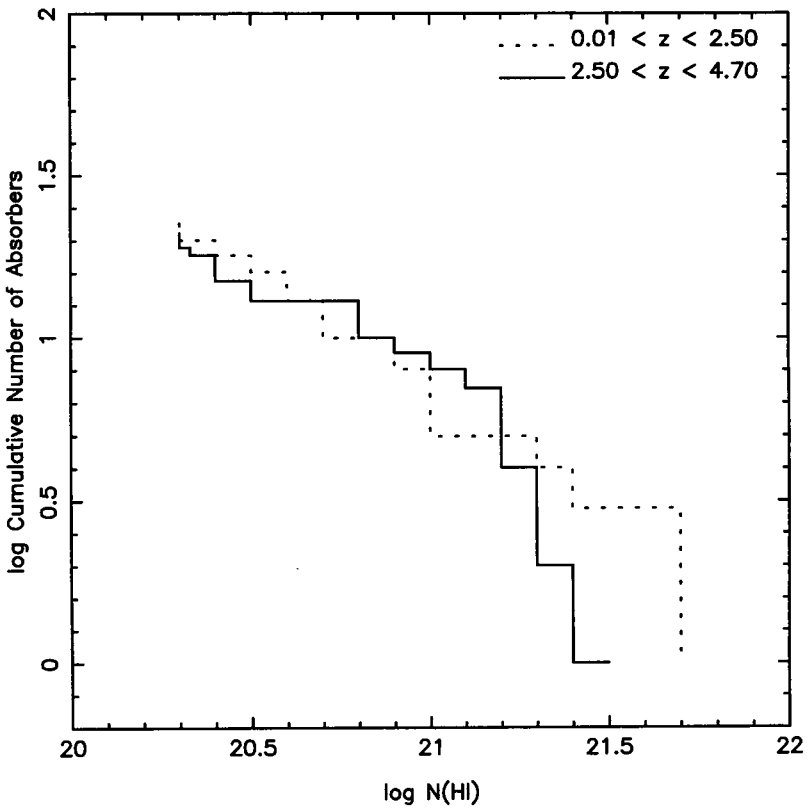

Figure 4. The cumulative H I column density distribution with the sample split in half at $z=2.5$. The damped Lyα systems with $z>2.5$ are shown by the solid line, and the absorbers with $z<2.5$ are shown by the dashed line. The higher redshift absorbers appear to have a slightly flatter slope up to $\log N_{\rm H\,I}=21$ and then a sharper drop in the number of very high column density systems, although a KS test shows that this is not a statistically significant difference.

test shows that this is not a statistically significant difference. The evolution with redshift in the slope of the column density distribution is also apparent when looking at the differential $f(N)$. LWT plotted this in three redshift bins, $z=[0.008, 1.5]$, $[1.5, 2.5]$ and $[2.5, 3.5]$. In the highest redshift bin there was a flattening of the column density distribution slope towards higher column densities. In Fig. 5 we have plotted our combined data set with this same binning, with the addition of one higher redshift bin $z=[3.5, 4.7]$. The flattening of the distribution function towards higher column density systems in the $z=[2.5, 3.5]$ bin in the LWT data is no longer pronounced. The most striking feature is the steepness of the distribution in the highest redshift bin. It is not just steeper due to an increase in the number of lower column density systems relative to the other bins. Even if 15–20 per cent of the candidate systems with $\log N_{\rm H\,I}\approx 20.3$ turn out not to be damped when observed at higher resolution, as we expect, this result still holds.

3.6 Results for a gamma distribution

There are two strong motivating factors to find an alternative model for describing the H I column density distribution. First, as shown in Section 3.4, there is direct evidence for an apparent variation in the power-law slope as a function of $N_{\rm H\,I}$. This implies that a higher order functional form other than a power law is needed to describe the column density distribution. Secondly, as noted in the introduction, with a power-law model the integral mass contained within damped Lyα systems is divergent for realistic values of β. This in turn means that it is impossible to assign a formal upper limit to any estimate of the neutral gas content of the early Universe. Consequently, following Pei & Fall (1995), we have chosen to model the data with a gamma distribution of the form

$$f(N, z)=(f_*/N_*)\,(N/N_*)^{-\beta}\mathrm{e}^{-N/N_*}, \qquad (7)$$

where f_* is the characteristic number of absorbing systems at the column density N_*, and N_* is a parameter defining the turnover, or 'knee', in the number distribution. Both f_* and N_* may in general vary with redshift, but for the moment we treat them as constants. This functional form is similar to the Schechter luminosity function (Schechter 1976). For $N\ll N_*$, the gamma function tends to the same form as the single power law $f(N)\propto N^{-\beta}$, whilst for $N\gtrsim N_*$, the exponential term begins to dominate.

We can understand how a gamma function might provide a better description of the damped Lyα data by considering the differential logarithmic slope, which is given by

$$\frac{\mathrm{d}\log f(N, z)}{\mathrm{d}\log N}=-\beta-\frac{N}{N_*}. \qquad (8)$$

As the column density approaches N_*, the slope begins to steepen and turns over rapidly at higher column densities; this is qualitatively similar to what we observe in Figs 3 and

4. Furthermore, the integral H I over the column density distribution (cf. equation 1) for $N_{\min} \ll N_*$ is now given by $f_* N_* \tau(2-\gamma)$, where τ denotes the standard gamma function. This function is bounded if $\gamma < 2$.

The maximum-likelihood technique outlined in Appendix A can readily be modified to incorporate this form. We note that the likelihood solution can be found over a two-dimensional grid of pairs of values of N_* and β, since the constant f_* can be directly computed using the constraint

$$m = \sum_{i=1}^{n} f_* \int_{N_{\min}}^{N_{\max}} \int_{z'_{\min}}^{z'_{\max}} f(N, z)\, \mathrm{d}z\, \mathrm{d}N, \qquad (9)$$

where m is the total number of observed systems. This is computationally much less intensive than doing a three-dimensional grid search. The results of a single functional fit to the entire data set are $\log N_* = 21.63 \pm 0.35$, $\beta = 1.48 \pm 0.30$, and $f_* = 1.77 \times 10^{-2}$. The log-likelihood function results with confidence contours are shown in Fig. 6(a). The best fit is overplotted on the differential form of $f(N)$ in Fig. 6(b), and on the cumulative distribution in Fig. 6(c). [The single-power-law form of $f(N)$ was shown fitted to the same data in Figs 2 and 3.] The differential form of the plots (Figs 2 and 6b) show little difference between the single-power-law and gamma-distribution fits. When displayed with the cumulative number of absorbers in Fig. 6(c), the gamma-distribution now clearly fits the entire data set with column densities $\log N_{\mathrm{H\,I}} \geq 20.3$. If the expected number of Lyman-limit systems are included in the fit, the results are $\log N_* = 21.36 \pm 0.15$, $\beta = 1.16 \pm 0.15$ and $f_* = 4.43 \times 10^{-2}$. This also provides a reasonable fit to the data, as shown in Figs 7(a)–(c).

4 NUMBER DENSITY EVOLUTION WITH REDSHIFT

Differential evolution in the number density of damped Lyα absorbers has been described by LWT and Wolfe et al. (1995). While the change in number density per unit redshift is consistent with no intrinsic evolution of the absorbers over the range $0 < z < 3.5$, they find that the systems with $\log N_{\mathrm{H\,I}} > 21$ disappear at a much faster rate from $z = 3.5$ to $z = 0$ than does the population of damped absorbers as a whole. We now examine the redshift evolution of the damped Lyα absorbers in our combined data set by determining the number density of absorbers per unit redshift, $\mathrm{d}N/\mathrm{d}z \equiv N(z)$. In a standard Friedmann universe for absorbers with cross-section πR_0^2 and number density Φ_0 per unit comoving volume

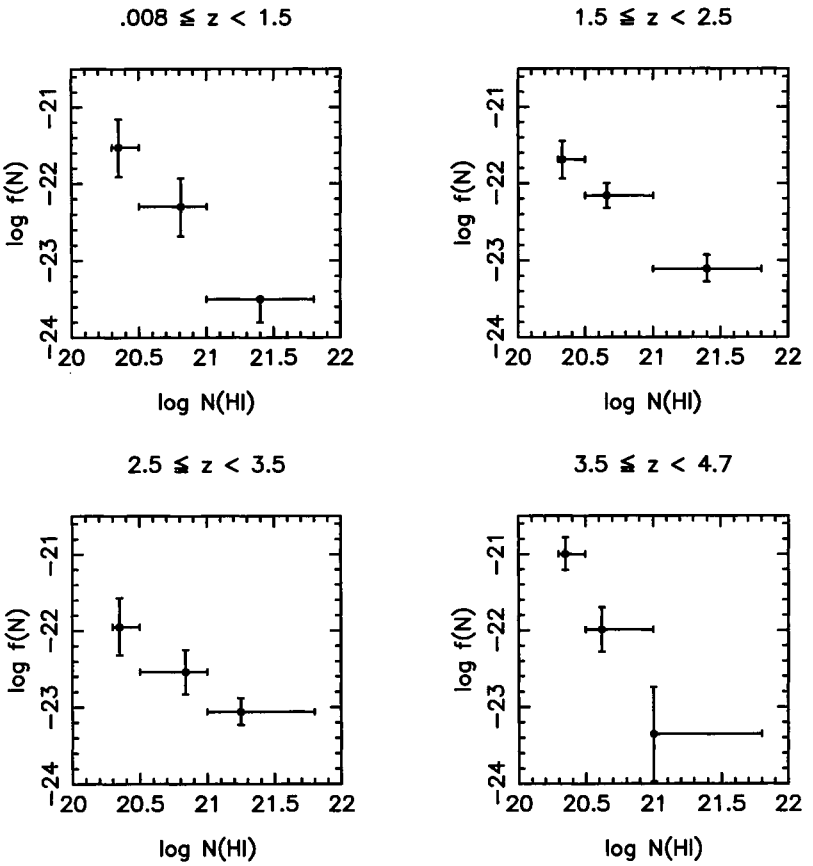

Figure 5. The log column density distribution function $f(N)$ versus the log column density $N_{\mathrm{H\,I}}$ plotted over four redshift ranges, $z = [0.008, 1.5]$, $[1.5, 2.5]$, $[2.5, 3.5]$ and $[3.5, 4.7]$, all binned in the column density ranges $\log N_{\mathrm{H\,I}} = [20.3, 20.5]$, $[20.5, 21.0]$ and $[21.0, 21.8]$. The gradual flattening of the distribution function from redshift $z = 0$ to $z = 3.5$ is evident. The most striking feature is the steepness of the distribution in the highest redshift bin. It is not just steeper due to a decrease in the highest column density systems ($\log N_{\mathrm{H\,I}} > 21$), but there is also an increase in the number of lower column density systems.

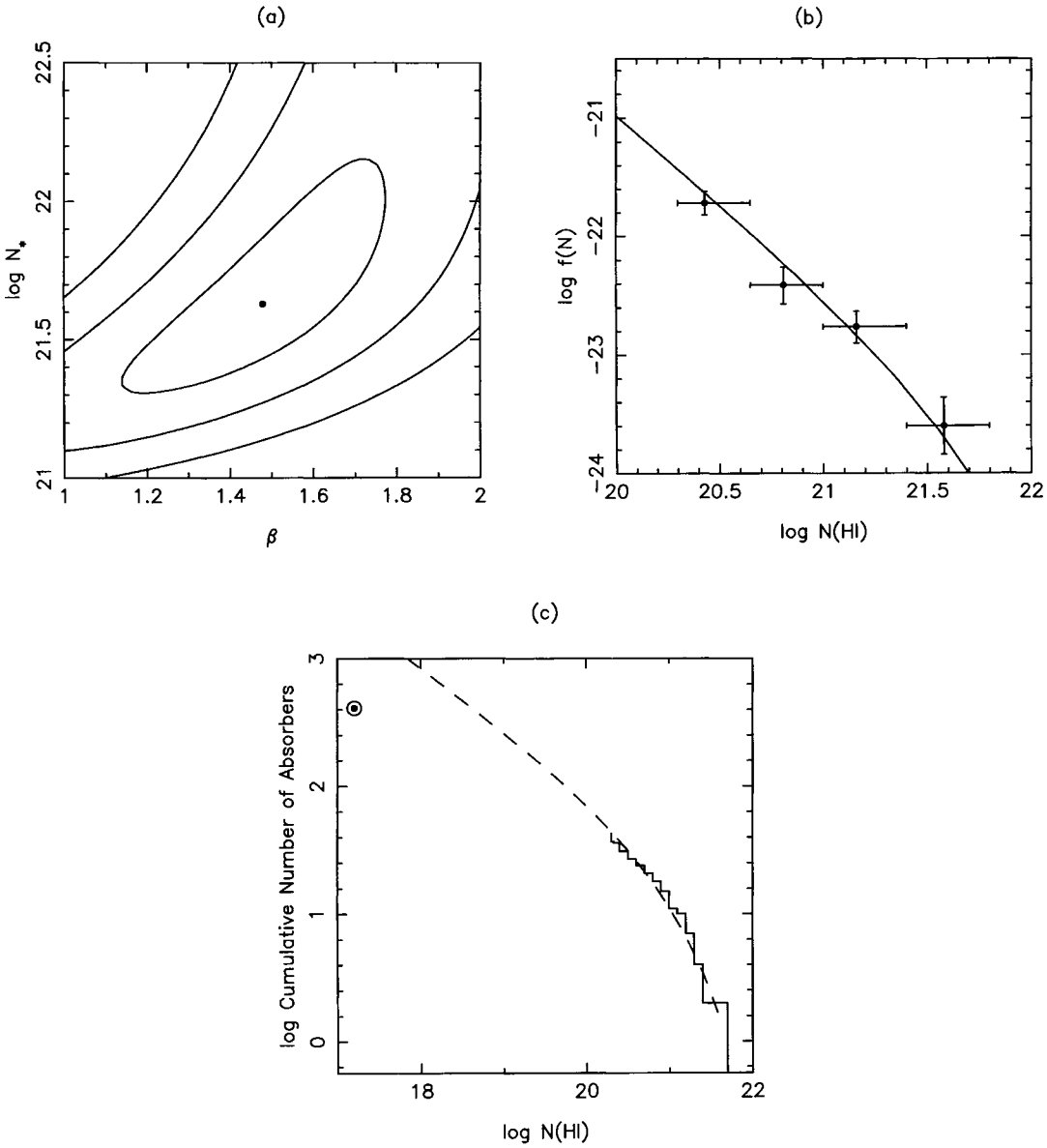

Figure 6. (a) The log-likelihood function for the gamma-distribution form of the column density distribution function, $f(N, z)=(f_*/N_*)(N/N_*)^{-\beta}\exp(-N/N_*)$. The >68.3, >95.5 and >99.7 per cent confidence contours are plotted for $\log N_*$ and β. The best-fitting values are $\log N_*=21.63$, $\beta=1.48$ and $f_*=1.77\times10^{-2}$, which is solved for analytically. (b) The gamma-distribution function, $f(N, z)=(f_*/N_*)(N/N_*)^{-\beta}\exp(-N/N_*)$, overplotted on the differential form of the column density distribution. The fit is to the entire data set, including the surveys from Paper II, WTSC, LWTLMH and LWT. The parameters for the fit are $\log N_*=21.63$, $\beta=1.48$ and $f_*=1.77\times10^{-2}$. (c) The cumulative distribution for $17.2\leq\log N_{\rm H\,I}\leq22$ as shown in Fig. 3(a) is now overplotted with the gamma-distribution form of the column density distribution function. The dashed line now clearly fits the entire distribution for $\log N_{\rm H\,I}\geq20.3$. The circled point is again the number of Lyman-limit systems that would be expected, given the redshift path covered in the damped Lyα surveys. This is not included in the fit.

$$N(z)=\Phi_0\pi R_0^2cH_0^{-1}(1+z)(1+2q_0z)^{-1/2}. \quad (10)$$

It is customary to represent the number density as a power law of the form

$$N(z)=N_0(1+z)^{\gamma}, \quad (11)$$

where $N_0=\Phi_0\pi R_0^2cH_0^{-1}$. This yields $\gamma=1$ for $q_0=0$ and $\gamma=1/2$ for $q_0=1/2$ for the case of no evolution with redshift in the product of the number density and cross-section of the absorbers (Sargent et al. 1980).

A maximum-likelihood fit to the data yields $N(z)=0.04(1+z)^{1.3\pm0.5}$, which is consistent with no intrinsic evolution, even though the value of γ is similar to that found for the Lyman-limit systems where evolution is detected at a significant level (Paper I; Stengler-Larrea et al. 1995). The log-likelihood function for γ and N_0 with >68.3 and >95.5 per cent confidence contours is plotted in Fig. 8. We also find redshift evolution in the higher column density systems, but with a decline in $N(z)$ for $z>3.5$. These results are displayed in Fig. 9. The entire data set is plotted as dashed

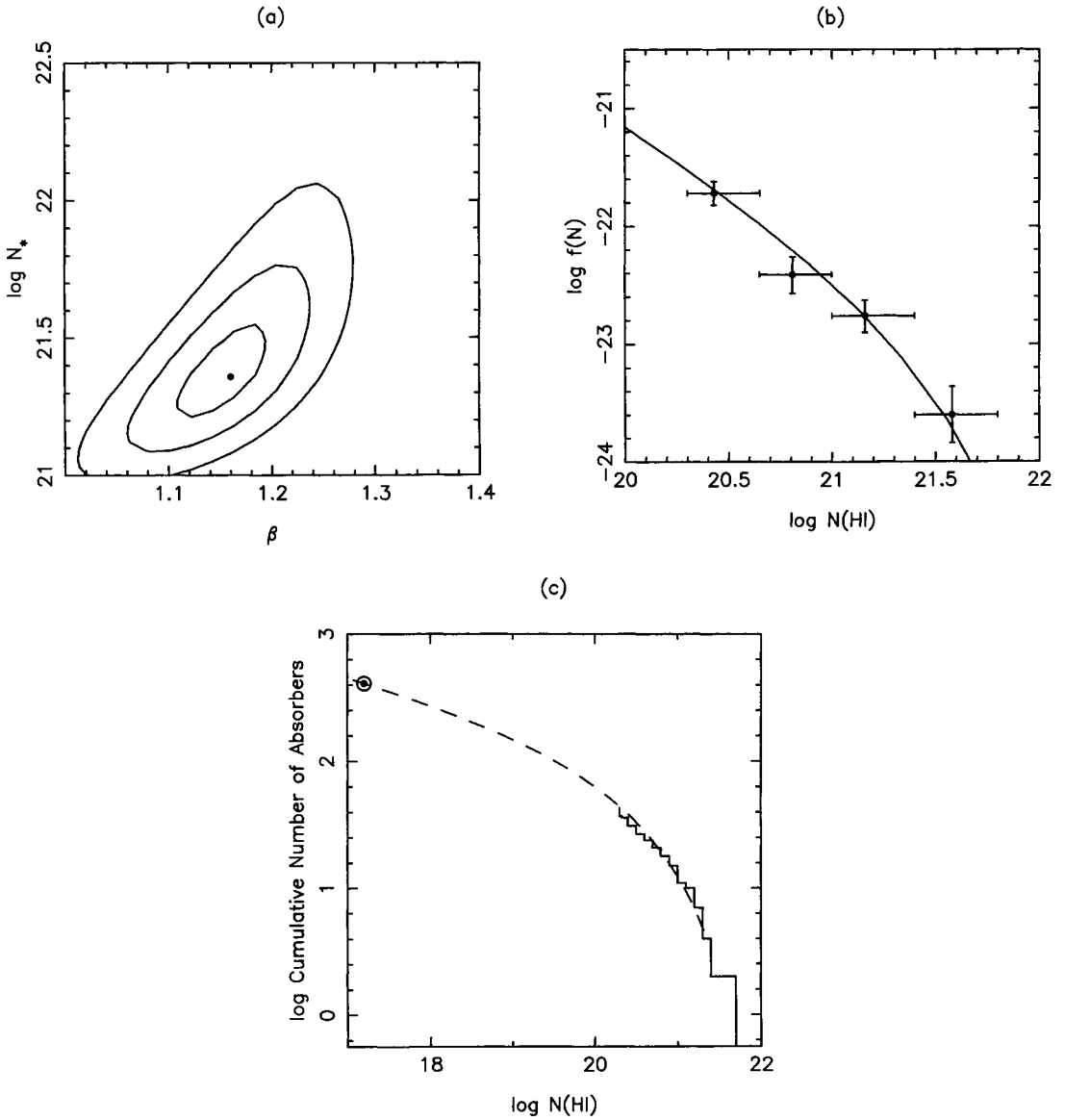

Figure 7. This figure shows the same data plotted in Fig. 6, but the fit includes the expected number of Lyman-limit systems, given the redshift path surveyed. (a) The log-likelihood function for the gamma-distribution form of the column density distribution function, $f(N,z)=(f_*/N_*)(N/N_*)^{-\beta}\exp(-N/N_*)$. The >68.3, >95.5 and >99.7 per cent confidence contours are plotted for $\log N_*$ and β. The best-fitting values are $\log N_*=21.36$, $\beta=1.16$ and $f_*=4.43\times10^{-2}$, which is solved for analytically. (b) The gamma-distribution function, $f(N,z)=(f_*/N_*)(N/N_*)^{-\beta}\exp(-N/N_*)$, overplotted on the differential form of the column density distribution. The fit is to the entire data set, including the surveys from Paper II, WTSC, LWTLMH and LWT. The parameters for the fit are $\log N_*=21.36$, $\beta=1.16$, and $f_*=4.43\times10^{-2}$. (c) The cumulative distribution for $17.2\leq\log N_{\rm H\,I}\leq22$ overplotted with the gamma-distribution form of the column density distribution function. The circled point is again the number of Lyman-limit systems that would be expected, given the redshift path covered in the damped Lyα surveys.

lines with the above fit. The results for only the absorbers with $\log N(\mathrm{H\,I})\geq21$ are shown as solid lines. Fig. 10 shows H I column density versus redshift, and the paucity of absorbers with $\log N_{\rm H\,I}>21$ at $z>4$ is apparent.

5 CONCLUSIONS

Three QSOs from the $z\gtrsim4$ APM survey have been observed at 0.8-Å resolution. Two have damped systems with confirmed H I column densities of $N_{\rm H\,I}\geq10^{20.3}$ atom cm^{-2}, with a third absorber falling just below this threshold. We have discovered the highest redshift damped Lyα absorber known at $z=4.383$ in QSO BR 1202−0725. The two systems with $N_{\rm H\,I}\geq10^{20.3}$ atom cm^{-2}, and the remaining nine candidate damped absorbers from the APM survey, have been combined with data from previous surveys to study the column density distribution and number density evolution for absorbers with $N_{\rm H\,I}\geq17.2$. If the H I column density distribution function is fitted with a power law, $f(N)=kN^{-\beta}$, we find evidence for breaks in the power law, flattening for $17.2\leq\log N_{\rm H\,I}\lesssim21$, and steepening for $\log N_{\rm H\,I}\gtrsim21$. The column density distribution function for the data with

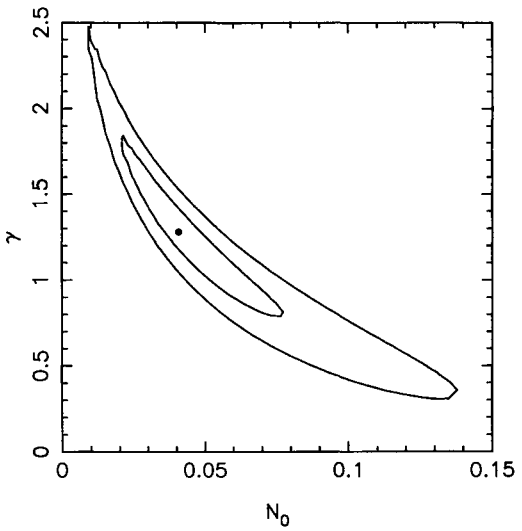

Figure 8. The >68.3 and >95.5 per cent confidence contours for the log-likelihood function are plotted for the number density per unit redshift of the damped absorbers. The best fit for the single power-law form $N(z)=N_0(1+z)^{\gamma}$ yields $\gamma=1.3\pm0.5$ and $N_0=0.04^{+0.03}_{-0.02}$ over the redshift range $0.008<z<4.7$.

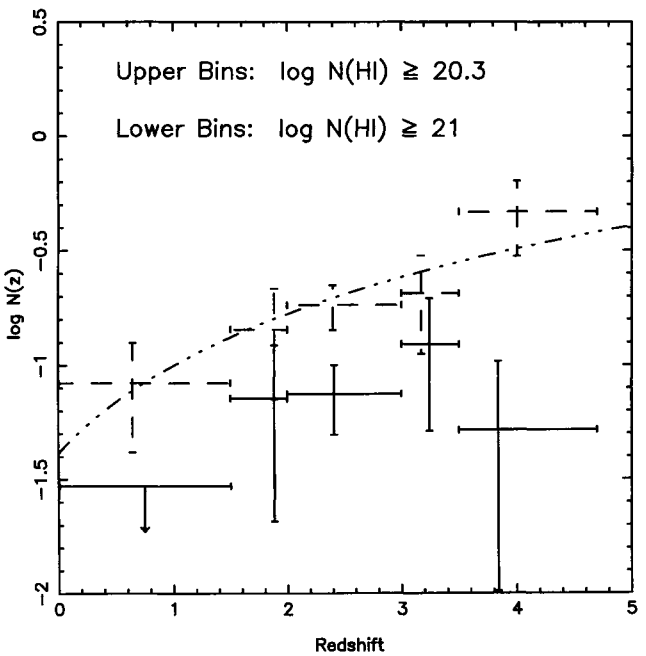

Figure 9. The number density of DLA per unit redshift, $N(z)$ versus z (absorption). The dashed bins show $N(z)$ for all the damped systems, and the solid bins for systems with $N(\mathrm{H\,I})\geq10^{21}$ atom cm^{-2}. A single power-law fit of $N(z)=0.04\,(1+z)^{1.3}$ is overplotted. This is consistent with no intrinsic evolution in the absorbers, even though the value of γ is similar to that found for the Lyman-limit systems where evolution is detected at a significant level (Paper I).

$\log N_{\mathrm{H\,I}}\geq20.3$ is better fitted with the gamma-distribution form $f(N)=(f_*/N_*)\,(N/N_*)^{-\beta}\exp(-N/N_*)$ with $\log N_*=21.63\pm0.35$, $\beta=1.48\pm0.30$ and $f_*=1.77\times10^{-2}$.

For the number density evolution of the damped absorbers ($\log N_{\mathrm{H\,I}}\geq20.3$) over the redshift range $0.008<z<4.7$,

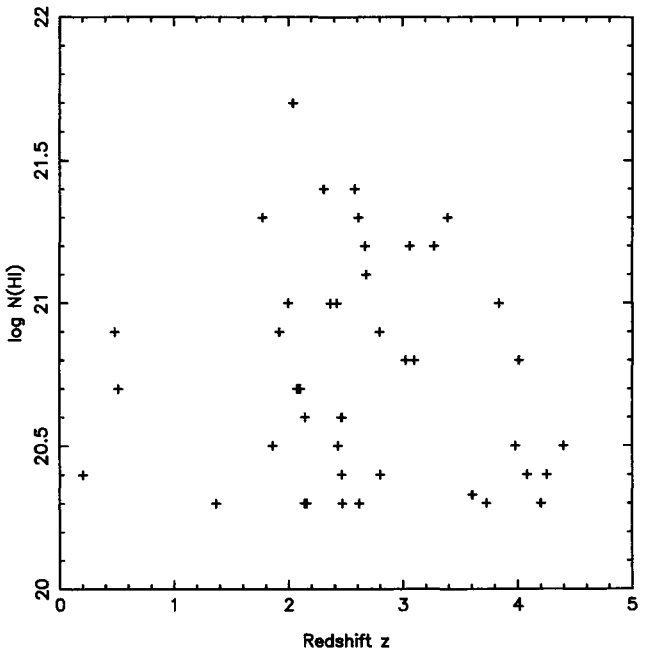

Figure 10. The H I column density of the damped Lyα absorbers is plotted versus absorption redshift. The paucity of absorbers with $\log N_{\mathrm{H\,I}}>21$ at $z>4$ is apparent.

we find the best fit of a single-power-law form for $N(z)=N_0(1+z)^{\gamma}$ yields $\gamma=1.3\pm0.5$ and $N_0=0.04^{+0.03}_{-0.02}$. This is consistent with no intrinsic evolution in the absorbers, even though the value of γ is similar to that found for the Lyman-limit systems where evolution is detected at a significant level. Evolution is evident in the highest column density absorbers with the incidence of systems with $\log N(\mathrm{H\,I})\geq21$ decreasing for $z\gtrsim3.5$.

ACKNOWLEDGMENTS

We thank Bob Carswell for providing software for and assistance with the data reduction and profile fitting of the spectra. LJSL acknowledges support from an Isaac Newton Studentship, the Cambridge Overseas Trust and a University of California President's Post-doctoral Fellowship. RGM acknowledges the support of the Royal Society.

REFERENCES

Bahcall J. N., Peebles P. J. E., 1969, ApJ, 156, L7
Carswell R. F., Morton D. C., Smith M. G., Stockton A. N., Turnshek D. A., Weymann R. J., 1984, ApJ, 278, 486
Cooke A. J., 1994, PhD thesis, Univ. Cambridge
Fall S. M., Pei Y. C., McMahon R. G., 1989, ApJ, 341, L5
Giallongo E., D'Odorico S., Fontana A., McMahon R. G., Savaglio S., Cristiani S., Molaro P., Trevesse D., 1994, ApJ, 425, L1
Lanzetta K. M., Wolfe A. M., Turnshek D. A., 1995, ApJ, 440, 435 (LWT)
Lanzetta K. M., Wolfe A. M., Turnshek D. A., Lu L., McMahon R. G., Hazard C., 1991, ApJS, 77, 1 (LWTLMH)
Lu L., Sargent W. L. W., Womble D. S., Barlow T. A., 1996, ApJ, 457, L1
Pei Y. C., Fall S. M., Bechtold J., 1991, ApJ, 378, 6
Pei Y. C., Fall S. M., 1995, ApJ, 454, 69

Petitjean P., Webb J. K., Rauch M., Carswell R. F., Lanzetta K. M., 1993, MNRAS, 262, 499
Pettini M., Boksenberg A., Hunstead R. W., 1990, ApJ, 348, 48
Pettini M., Smith L. J., Hunstead R. W., King D. L., 1994, ApJ, 426, 79
Rauch M., Carswell R. F., Robertson J. G., Shaver P. A., Webb J. K., 1990, MNRAS, 242, 698
Sargent W. L. W., Young P. T., Boksenberg A., Tytler D., 1980, ApJS, 42, 41
Sargent W. L. W., Steidel C. C., Boksenberg A., 1989, ApJS, 79, 703
Schechter P., 1976, ApJ, 203, 297
Schechter P., Press W. H., 1976, ApJ, 203, 557
Stengler-Larrea E. A. et al., 1995, ApJ, 444, 64
Storrie-Lombardi L. J., McMahon R. G., Irwin M. J., Hazard C., 1994, ApJ, 427, L13 (Paper I)
Storrie-Lombardi L. J., McMahon R. G., Irwin M. J., Hazard C., 1996, ApJ, 468, 121 (Paper II)
Storrie-Lombardi L. J., McMahon R. G., Irwin M. J., 1996, MNRAS, in press (Paper IV)
Tytler D., 1987, ApJ, 321, 49
Wampler E. J., Williger G. M., Baldwin J. A., Carswell R. F., Hazard C., McMahon R. G., 1996, A&A, in press
Williger G. M., Baldwin J. A., Carswell R. F., Cooke A. J., Hazard C., Irwin M. J., McMahon R. G., Storrie-Lombardi L. J., 1994, ApJ, 428, 574
Wolfe A. M., 1987, Proc. Phil. Trans. Roy. Soc., 320, 503
Wolfe A. M., Turnshek D. A., Smith H. E., Cohen R. D., 1986, ApJS, 61, 249 (WTSC)
Wolfe A. M., Lanzetta K. M., Foltz C. B., Chaffee F. H., 1995, ApJ, 454, 698

APPENDIX A: MAXIMUM-LIKELIHOOD ANALYSIS

Using equation (5) for the column density distribution function, the damped Lyα absorbers will be found to be randomly distributed according to this function along the QSO line of sight in N–z space. If the space is divided into m cells, each of volume δv, the expected number of points in cell i is given by

$$\phi_i = f(N, z)_i \delta v. \tag{A1}$$

The probability of observing x_i points in cell i is

$$p(x_i) = \mathrm{e}^{-\phi_i} \frac{\phi_i^{x_i}}{x_i!}. \tag{A2}$$

The likelihood function for QSO$_j$, taking the product over all the cells, is then

$$L_j = \prod_{i=1}^{m} p(x_i) = \prod_{i=1}^{m} \mathrm{e}^{-\phi_i} \frac{\phi_i^{x_i}}{x_i!}. \tag{A3}$$

If the volume of each cell δv becomes very small, such that there is either 1 or 0 points in each cell,

$$x_i = \begin{cases} 1, & \text{if DLA detected,} \\ 0, & \text{if none detected,} \end{cases}$$

then the likelihood can be rewritten separating out the terms for full and empty cells. For $m = g$ empty cells $+ p$ full cells,

$$L_j = \prod_{i=1}^{g} \mathrm{e}^{-\phi_i} \prod_{j=1}^{p} \mathrm{e}^{-\phi_j} \phi_j = \prod_{i=1}^{m} \mathrm{e}^{-\phi_i} \prod_{j=1}^{p} \phi_j. \tag{A4}$$

Taking the log of the likelihood function, we obtain

$$\begin{aligned} \log L_j &= \sum_{i=1}^{m} -\phi_i + \sum_{j=1}^{p} \ln \phi_j \\ &= \sum_{i=1}^{m} -f(N, z)_i \delta v + \sum_{j=1}^{p} \ln f(N, z)_j + p \ln \delta v \end{aligned} \tag{A5}$$

(cf. Schechter & Press 1976). Ignoring the constant terms, in the limit where $\delta v \to 0$ this becomes

$$\begin{aligned} \log L_j &= -\int_{z_{\min}}^{z_{\max}} \int_{N_{\min}}^{N_{\max}} f(N, z)\, \mathrm{d}N\, \mathrm{d}z + \sum_{j=1}^{p} \ln f(N, z)_j \\ &= -\int_{z_{\min}}^{z_{\max}} \int_{N_{\min}}^{N_{\max}} kN^{-\beta}(1+z)^{\gamma}\, \mathrm{d}N\, \mathrm{d}z \\ &\quad + \sum_{j=1}^{p} \ln [kN^{-\beta}(1+z)^{\gamma}]. \end{aligned} \tag{A6}$$

To obtain the overall log likelihood for n QSOs, we evaluate the integrals in equation (A6) and additively combine the log Ls, resulting in

$$\begin{aligned} \log L = \sum_{i=1}^{n} \Bigg\{ &\frac{kN_{\min}^{1-\beta}}{(1-\beta)(1+\gamma)} [(1+z_{\mathrm{em}}^{i})^{1+\gamma} - (1+z_{\min}^{i})^{1+\gamma}] \\ &+ p \ln k + \sum_{j=1}^{p_i} [-\beta \ln N_j + \gamma \ln (1+z_{\mathrm{dla}}^{j})] \Bigg\}, \end{aligned} \tag{A7}$$

where p_i is the number of detected DLAs in QSO$_i$, and $N_{\min}$ is the minimum column density.